Architecture
Image Studies

Vol.7, Issue 1, pp.2731-2744, 2026
DOI: https://doi.org/10.62754/ais.v7i1.1304

https://journals.ap2.pt/index.php/ais/index

Seismic Performance of an Earth Dam Strengthened with HDPE Geogrids by Finite Element Analysis

Iman Hameed Al-Shahrastani[1], Atheer Zaki Al-Qaisi[2]

Abstract

Earth dams constructed in seismic areas are very susceptible to the strong ground shaking, particularly when in near-full reservoir conditions that cause increase of system requirement through hydro-mechanical interaction. The present article studies the dynamic response of Al-Adhaim Dam during El-Centro earthquake record (PGA = 0.30 g) at full reservoir level (EL = 143 m) with and without buttressing from high-density polyethylene (HDPE) geogrid during its service life. A fully coupled flow–deformation finite-element formulation was used for the analysis of the seismic displacement, acceleration amplification, stress redistribution, pore-pressure response, seepage behavior and overall stability. Results show that the unretrofitted dam undergoes large seismic-induced deformations of 0.33 m and peak crest acceleration amplifications up to 0.78 g, which result in a well FOS<1.0), indicating an unstable condition due to seismic loading. After reinforcement, the maximum displacements at the critical downstream zone are decreased by over 97% (from ~0.30 m to 8×10^{-3} m), whereas the factor of safety increases to stabilized values in the range between 1.69 and 1.83 for all reinforcements conditions. A one-way ANOVA test indicates that both reduction of the displacement ($p < 10^{-4}$) and improving factor of safety ($p < 10^{-4}$) are statistically significant, indicating that these improvements do not result from numerical variability but are due to the mechanical effect contributed by geogrid system. The stress analysis shows that the level of confinement in downstream shell is increased while pore pressure response and seepage pattern become constant without any ill effect from the reinforcement. All these results prove that HDPE geogrid reinforcement has been an effective and statistically proved approach for reinforcing and improving the seismic resistance of earth dams under extremely strong ground motion, which provides a reliable theoretical basis for seismic strengthening design of embankment dam in seismically high-risk areas.

Keywords: *Numerical Modeling, Earth dams, Earthquake, Al-Adhaim Dam, HDPE*

Introduction

Earth dams constitute a critical class of hydraulic infrastructure worldwide, providing essential services for water storage, flood mitigation, and irrigation, particularly in regions where geological and geomorphological conditions favor embankment-based systems. The long-term performance and safety of such structures are governed by the complex interaction between the geotechnical properties of embankment materials, the mechanical and hydraulic characteristics of foundation strata, and the spatially and temporally variable seepage processes occurring within the dam body and its foundation (Adamo, 1985). These interactions become increasingly critical under extreme loading conditions, where deformation mechanisms, pore water pressure redistribution, and stability margins may evolve in a highly nonlinear manner. In earth-fill dams constructed on stratified foundations, variations in soil stiffness, permeability, and hydraulic conductivity exert a pronounced influence on deformation patterns, stress redistribution, and pore pressure development, ultimately controlling structural stability (Akbaş, 2015). The Al-Adhaim Dam represents a representative case of such systems, as it is founded on alternating marl and sandstone formations that require careful geotechnical characterization to ensure safe operation under both normal reservoir conditions and extreme events. Geographically, the dam is located in eastern Iraq within Diyala Governorate (38°23′25.4″ N, 45°48′43″ E), a region

[1] Department of Water Resources Management Engineering, College of Engineering, Al-Qasim Green University, Babylon 51013, Iraq. Email: iman00hameed@gmail.com (corresponding author).
[2] Department of Water Resources Management Engineering, College of Engineering, Al-Qasim Green University, Babylon 51013, Iraq.

influenced by the Zagros–Bitlis seismic belt and characterized by moderate to high seismic hazard **(Fig. 1)** (Hussain et al., 2022).

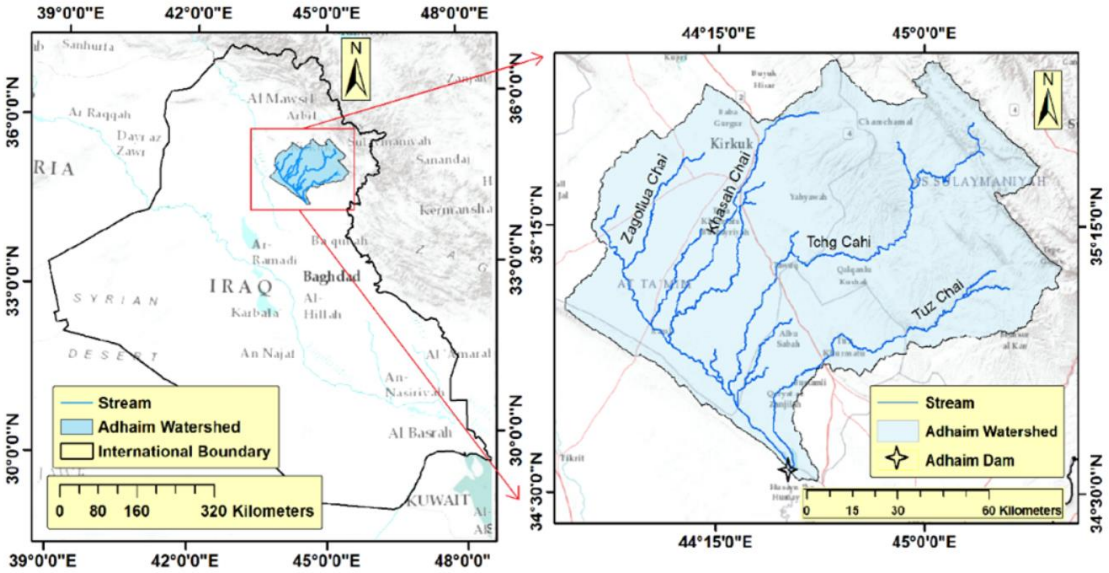

Fig 1: Al-Adhaim Dam location (Al-Labban, 2007).

This tectonic influence requires robust stability analyses, which take into explicit account hydro-mechanical coupling and seismic loading. The numerical method of finite elements (FEM) has proved to be an essential tool for the analysis of hydraulic and mechanical behavior in earth dams, particularly in the assessment of coupled hydrostatic–deformation processes under static and dynamic conditions (Chimdesa et al., 2023). The FEM simulations accuracy is highly dependent on the mesh resolution, element type and discretization approach, which determine their ability to represent hydraulic gradients, stress distribution and localized deformations in a heterogeneous dam–foundation system. These aspects are particularly relevant for zoned embankments like the Al-Adhaim Dam, with a central core of clay complemented by upstream and downstream kernels, filter zones and transition ones, as well as by a stratified marl–sandstone foundation **(Fig. 2)** (Fallah et al., 2015). With these conditions, coarser meshes or low-order elements could fail to represent seepage paths, localization and strain near the core of deformed foundation masses and mechanisms for stress transfer in the foundation layers. However, despite the wide application of FEM in dam engineering, it continues to be a research gap that the influence of mesh setting on predicted deformation, seepage behavior and stability indices should be systematically quantified for earth dams with realistic hydraulic boundary conditions. In particular, sensitivity studies with respect to the factor of safety (FOS) and hydro-mechanical response due to mesh discretization have rarely been considered for stratified dam–foundation systems subjected to more than one reservoir level. Water level of EL = 143 m for Al-Adhaim Dam represent different hydraulic states, which have direct impact on the seepage regimes and stress distributions (Ghalib et al., 1974). Therefore, the purpose of this study is to analytically examine the impact of FEM mesh pattern on the static hydro-mechanical behavior on Al-Adhaim Dam with focus on the deformation mechanisms, groundwater seepage states and corresponding SFs. The study, which quantifies numerical sensitivity under practical material and boundary conditions, seeks to recommend a set of pragmatic modeling guidelines for earth-fill dams that promote prediction confidence and facilitate risk-informed design and performance assessment. Although due to 2D idealization and material behavior assumptions, the underlying limitations of such a methodology are inevitable; however, this provides the first step towards developing tools to improve numerical stability for dam engineering practice, as well as provide a rigorous platform for subsequent dynamic and reinforcement analysis **(Fig. 2)** (Ghalib et al., 1974)

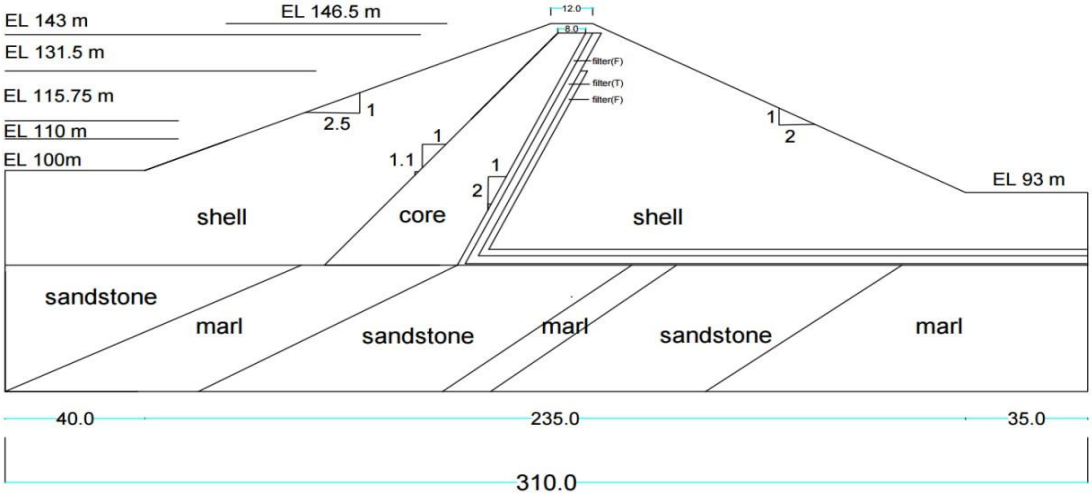

Fig 2: Cross-sectional schematic diagram of Al-Adhaim Dam showing the zoned earth-fill structure, core, shell, filter layers, and foundation geology (Ministry of Water Resources, 1994).

Data Collection

The study utilized both primary and secondary data sources. The data collected consisted of a visual inspection of the existing physical conditions of the dam, recording the upstream and downstream elevations, and interviews with resident engineers, hydrogeologists, dam operators, and stakeholders within the affected area to capture operational status as well as perceptions regarding performance issues (Novak et al., 2007). The primary input of the modelling process was secondary data, which were supplied by the General Directorate for Dams and Reservoirs, Ministry of Water Resources, Iraq. These included the initial design files, geotechnical data, laboratory-tested foundation materials, geologic reports, project completion and topographic maps, and structural drawings of the dam. Information on the reservoir's key characteristics (e.g., elevations, storage capacities, and surface area) was also collected from these datasets and is provided in **(Table 1),** where the main operational and design water levels used for numerical simulations are presented. **(Table 1)**, clearly depicts the design water level (143 m), the operating water level (131.5 m), and the dead water level (110 m). They are important for describing the boundary conditions and hydraulic loads in the numerical model. The engineering soil parameters in this study were obtained from the general geological and geotechnical investigation report (1994), which includes the necessary inputs for the correct representation of material behavior in FE analyses (Novak et al., 2017).

Table 1. Reservoir Elevation Levels and Corresponding Storage Characteristics

Item	Elevation (EL), m	Storage (Mm^3)	Surface Area (km^2)
Dam top level	146.5	—	—
Design water level	143	3,750	270
Operation level	131.5	1,600	135
Irrigation and power level	118.0	450	52
Dead water level	110.0	160	28
Current water level (April 2024)	111.0	130	—
Diversion (bottom outlet) invert level	86.16	—	—

Results and Discussion

Dam Response before Reinforcement

The seismic performance of Al-Adhaim Dam under the El-Centro earthquake with a peak ground acceleration of 0.30 g at the maximum reservoir level (EL = 143 m a.m.s.l.) was evaluated using fully coupled dynamic consolidation analysis. This approach captures the interaction between deformation, stress redistribution, and transient seepage flow, enabling a realistic assessment of dam behavior under strong seismic excitation.The unreinforced dam exhibits pronounced deformation

demand, dominated by horizontal motion. As shown in the time histories of total displacement magnitude **(Fig. 3 and Fig 4)** (Talukdar et al., 2012).the maximum nodal displacement reaches approximately 0.33 m, with values at selected monitoring nodes ranging between 0.183 m and 0.33 m **(Table 2)**.The largest displacements are observed in the intermediate and downstream regions, reflecting reduced confinement and concentration of shear strains in these zones. Horizontal displacement components **(Fig. 5 and Fig 6)** govern the response, whereas vertical displacements **(Fig. 7)** remain comparatively small (≈ 0.04–0.05 m), indicating that seismic deformation is primarily controlled by inertia-driven sliding mechanisms rather than settlement or uplift **(Table 2)** (Talukdar et al., 2012).

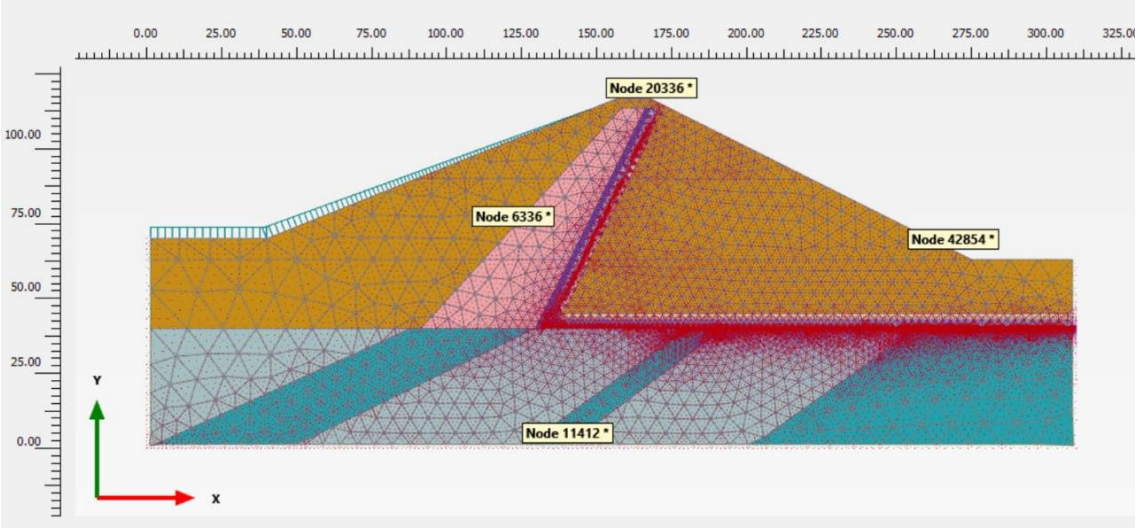

Fig 3: Finite-element mesh and numerical model configuration of Al-Adhaim Dam showing representative monitoring nodes (Nodes 20336, 6336, 11412, and 42854) used for extracting dynamic response under seismic loading

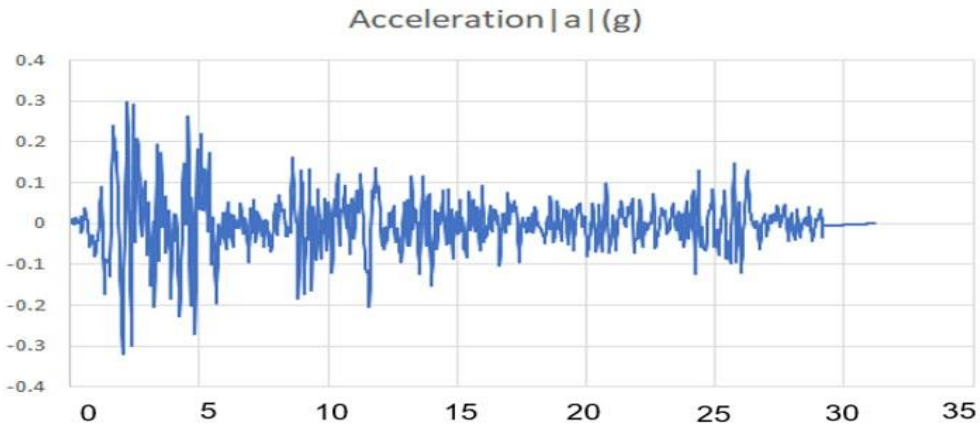

Fig 4: Time history of total acceleration magnitude | a | |a| (g) recorded at the selected monitoring point under seismic loading.

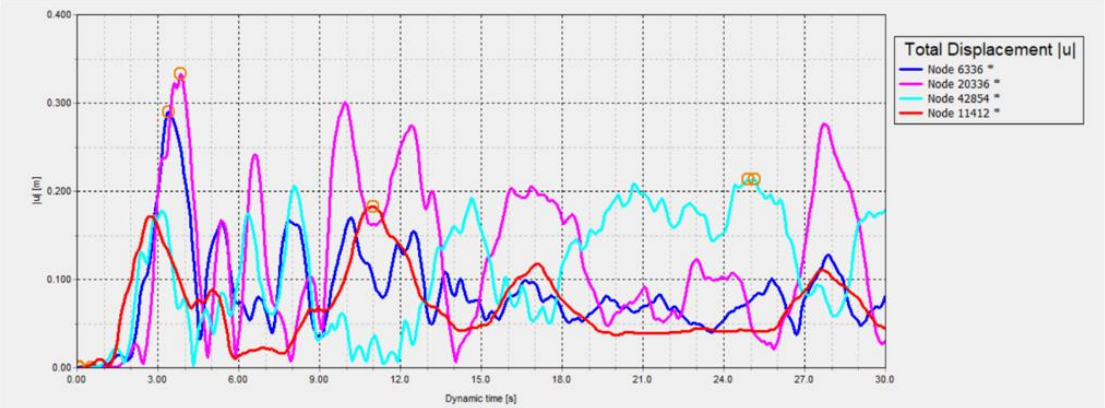

Fig 5: Time histories of total displacement magnitude |u| at selected monitoring nodes

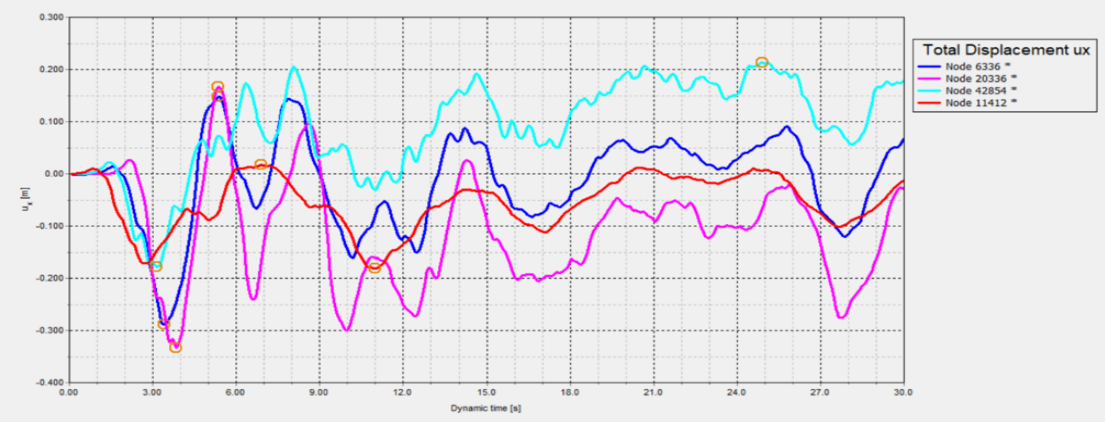

Fig 6: Time histories of horizontal displacement component (u_x) at selected monitoring nodes

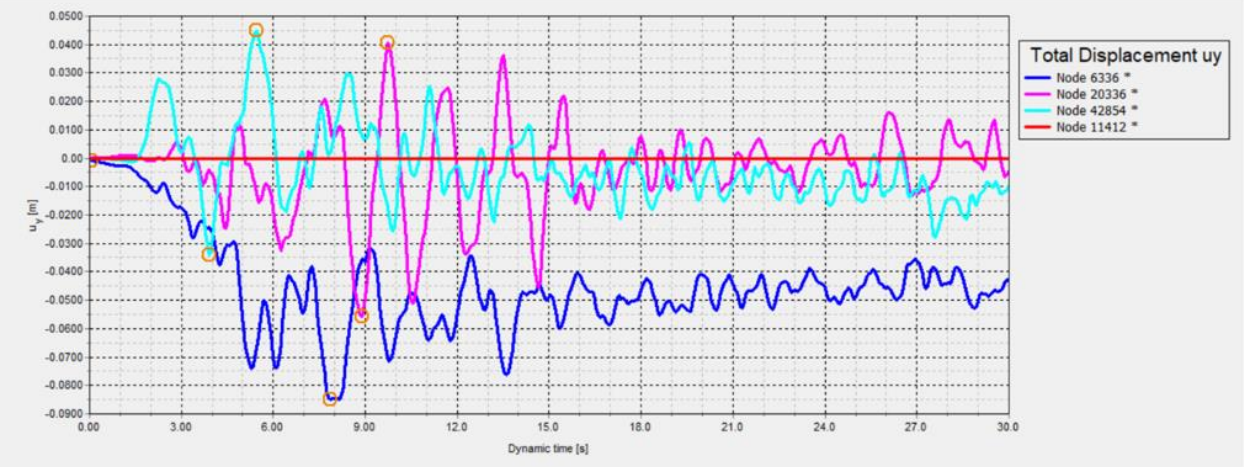

Fig 7: Time histories of vertical displacement component (u_Y) at selected monitoring nodes

Acceleration response shows significant spatial amplification over the embankment. The absolute value of the total acceleration |a| **(Fig. 8)** is larger than the input PGA, with a maximum of about 0.775 g in the top embankment , while the bottom part and middle part show accelerations between 0.345 g and 0.723 g **(Table 2)** (Abbas et al., 2021). The response for the horizontal acceleration component **(Fig. 9)** is greater than that for the vertical one **(Fig. 10)**, which takes part in multi-direction dynamic taxing, especially in the central core and upper shell. Information In this study, we show that such

amplification results from the combined action of modal interaction, impedance contrast between dam zones and vertical wave propagation **(Table 2)** (Abbas et al., 2021).

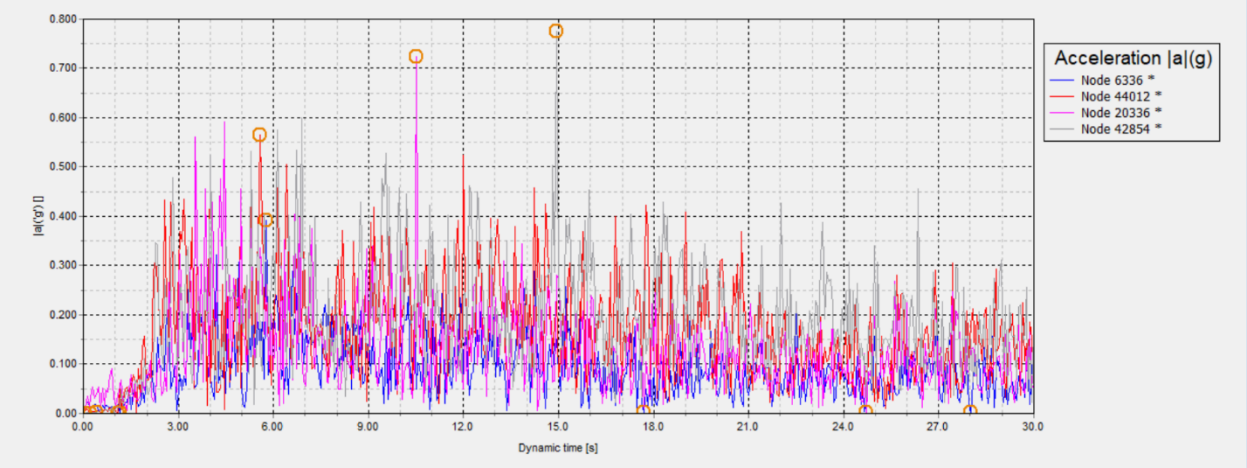

Fig 8: Time histories of total acceleration magnitude |a| at selected monitoring nodes under dynamic seismic loading.

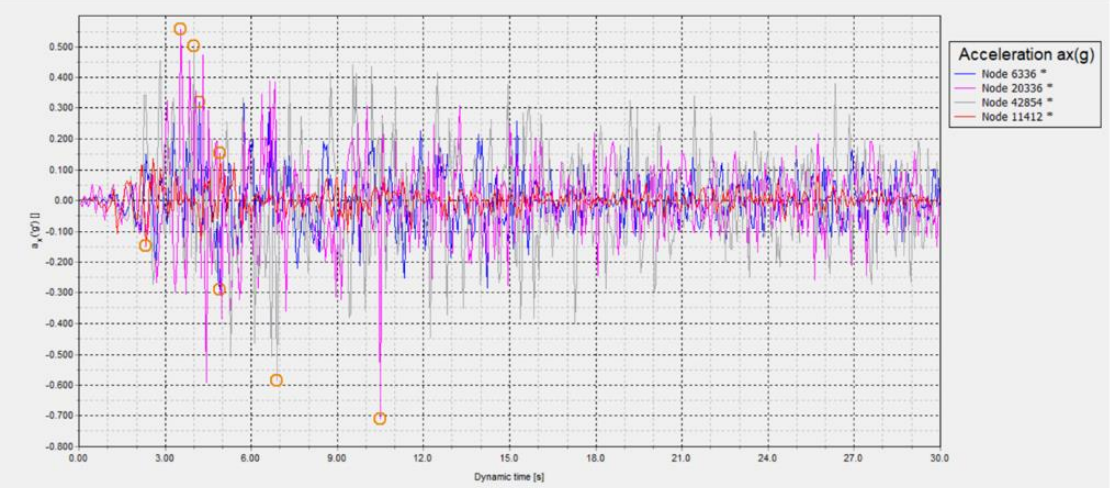

Fig 9: horizontal acceleration (a_x) response at selected nodes: under dynamic loading.

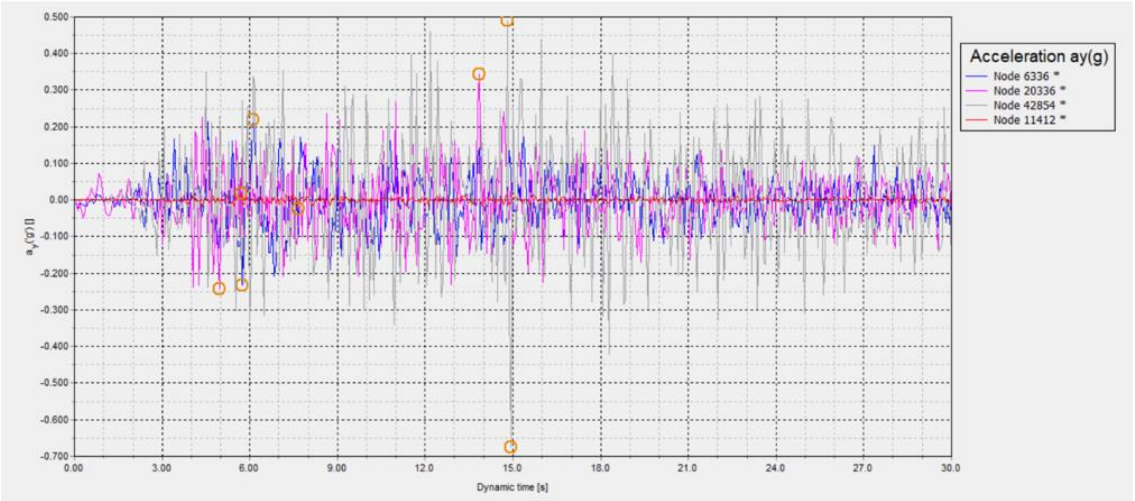

Fig 10: vertical acceleration a_x response at selected nodes: under dynamic loading.

The stress states are mainly compressive in all along the body of the dam. Cartisian stress time results **(Fig. 11)** showed maximum horizontal stresses of about −1279 kN/m² and vertical stresses of up to −2022 kN/m² at deeper stress stations **(Table 2)**. Localized small tensile stresses do develop near the crest ($\sigma_{xx} \approx +7$ kN/m²), but they are not large enough to reach a structural cracking or damage level. This substantiates the fact that the dam possesses an overall compressive stress regime under strong seismic excitations **(Table 2)** (Adamo, 1985).

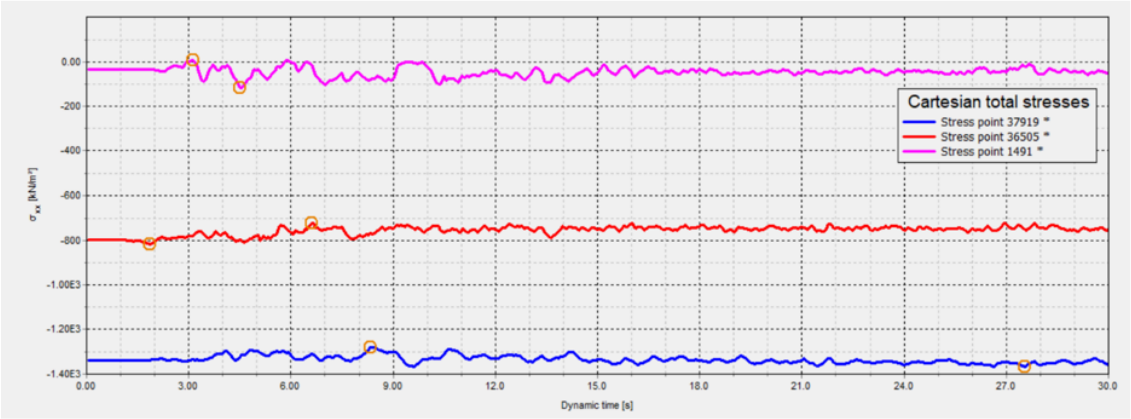

Fig 11: Time histories of Cartesian total horizontal stress σ_{xx}

The hydraulic response corresponds to the steady pore pressure. Active and excess pore pressures **(Fig. 12 and Fig.13)** that do not become unduly high (maximum of some 63.8 kPa) point to limited time-dependent and peaktime duration of excess pressure with the effective stress at times adjusted by negative total active pore pressures reaching −341 kPawhich signal temporary suction with dynamic stiffening effects. There is no indication of a continuous buildup of progressive pore-pressure, liquefaction or hydraulic failure. Still the groundwater flow velocity and seepage discharge are all within acceptable range, this means that the seismic response is a mechanical controlling behavior rather than a hydraulically driven one **(Table 2)** (Al-Amshawee, 2014).

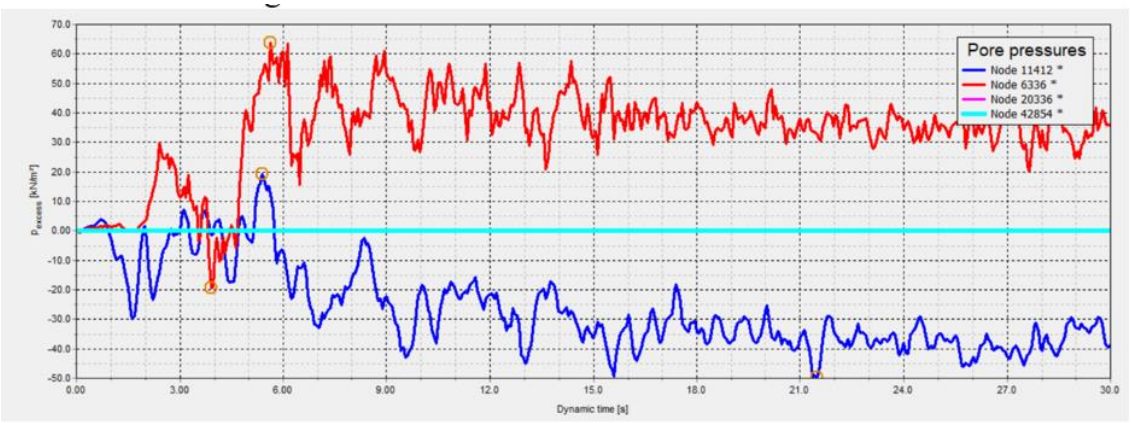

Fig 12: Time histories of excess pore water pressure (P_excess) at selected monitoring nodes under dynamic seismic loading.

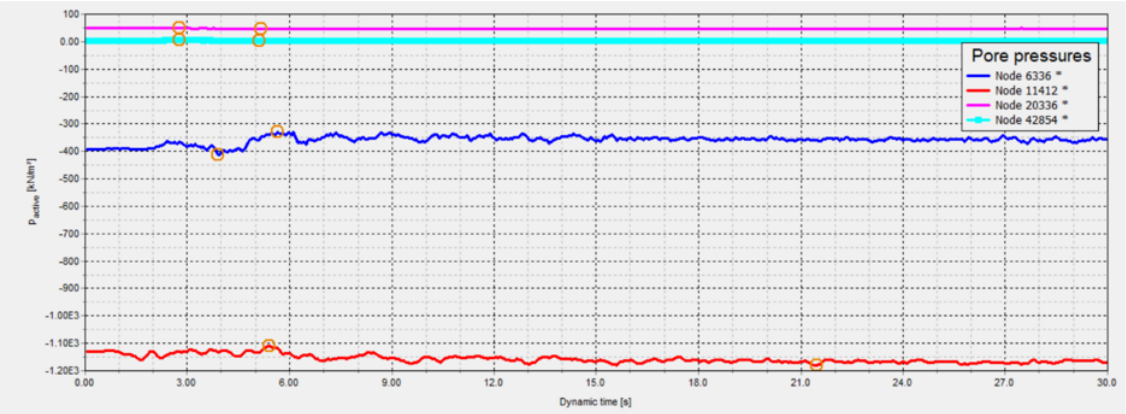

Fig 13: Time histories of active pore water pressure (P_active) at selected monitoring nodes

Overall, despite the severe dynamic demand imposed by the El-Centro earthquake, the unreinforced dam maintains elastic–plastic stability with controlled ductility, stable stress redistribution, and limited pore pressure buildup. However, the relatively large displacement amplitudes, particularly along the downstream slope, highlight the serviceability vulnerability of the dam under extreme seismic loading and justify the need for reinforcement measures **(Table 2)** (Al-Hadidi et al., 2021).

Table 1. Integrated Maximum Dynamic Response of Al-Adhaim Dam under El-Centro Earthquake (PGA = 0.30 g, Reservoir Level = 143 m)

Response Parameter	Node 6336	Time (s)	Node 20336	Time (s)	Node 24854	Time (s)	Node 11412	Time (s)
Total displacement, |u| (m)	0.330	3.78	0.290	3.30	0.211	24.84	0.183	10.80
Horizontal displacement, u_x (m)	0.161	5.28	0.144	5.28	0.212	24.22	0.014	6.84
Vertical displacement, u_Y (m)	0.048	~6.0	0.041	~5.4	0.045	~27.96	0.044	~27.96
Total acceleration, |a| (g)	0.392	5.70	0.723	10.44	0.775	14.88	0.345	5.58
Horizontal acceleration, a_x (g)	0.280	4.14	0.557	3.84	0.501	4.02	0.490	14.84
Vertical acceleration, a_Y (g)	0.219	6.06	0.253	13.86	0.037	4.86	0.018	5.70
Excess pore pressure, P_excess (kPa)	63.77	5.64	19.40	5.40	0.00	—	0.00	—
Active pore pressure, P_active (kPa)	−341.48	5.64	−111.40	5.34	+48.25	2.76	+4.66	2.70

Effect of Downstream Reinforcement Using HDPE Geogrid

To reduce the effect of seismic-induced deformation and enhance slope stability, Al-Adhaim Dam downstream face was wrapped with high-density polyethylene (HDPE) geogrid. reinforcement structure take six layers geogrids which were horizontally paved on the downstream of dam shell crossing potential slip surface to delay the relative motion of them. Various reinforcement patterns were analyzed for different geogrid lengths (30–70 m) and vertical spacing among grids (2 and 4 m) and The selected geogrid is assigned a tensile strength (EA) of 60 KN/m² .A satisfactory improvement of the seismatic performance with respect to non-strengthened configuration is highlighted by dynamic response analyses of strengthened configurations as presented in **(Fig.14 and Fig. 15)** (Al-Janabi et al., 2020).

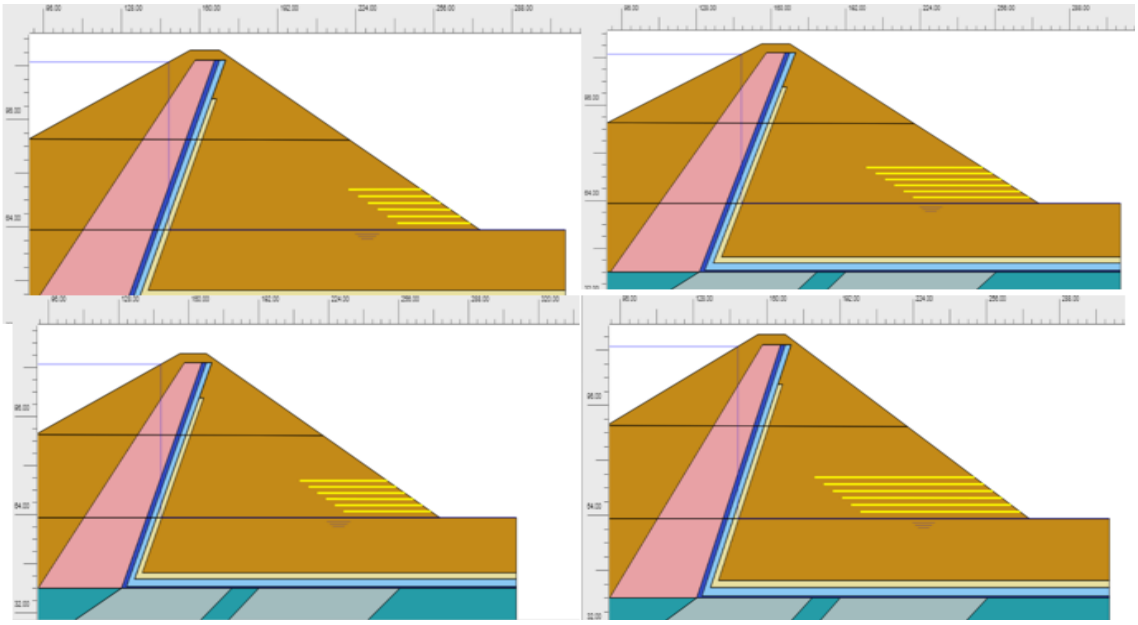

Fig 14. Numerical configurations of the Al-Adhaim Dam illustrating downstream HDPE geogrid reinforcement layouts with varying embedment lengths and vertical spacings.

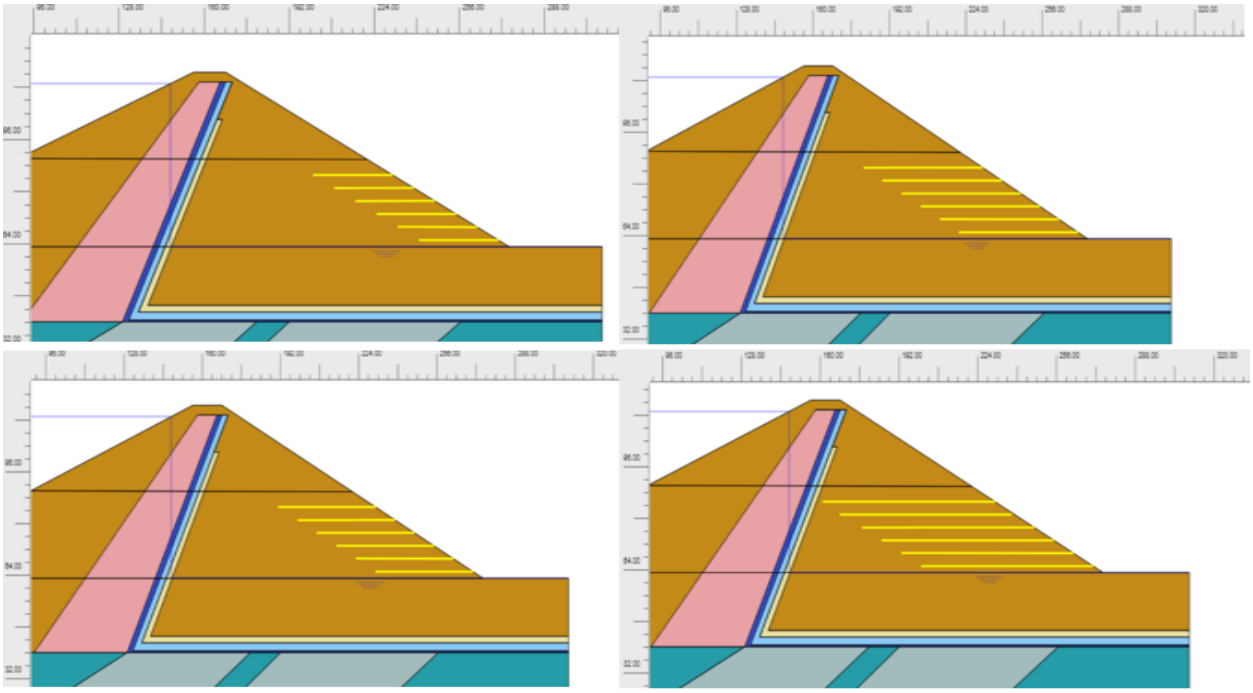

Fig 15. Numerical model configurations of the Al-Adhaim Dam illustrating representative downstream slope HDPE geogrid reinforcement layouts with varying embedment lengths and vertical spacings.

In the critical downstream monitoring node as presented in (Part G), the time history of total displacement demonstrates considerable reduction in both the displacement magnitude and vibration amplitude after strengthening . In this unreinforced state, the dam exhibits displacement of the order 10^{-1} m **(Fig. 16)** (Al-Nedawi et al., 2020). For a based condition the displacement is controlled to be about (7.8–8.1 × 10^{-3}) m and is an improvement in the range of one order-of-magnitude under such conditions. The determined FOS with the downsizing method is greatly increased due to reinforcement.Optimal design by the combination of six geogrid layers and 2 m spacing to lengths ranging between 30–50 m accomplish FOS values within range of 1.696–1.758 without any appreciable displacement. Although a 70 m geogrid length provides the highest FOS (≈ 1.827), the increase in relation to higher construction costs would be less economic.For 4 m spacing cases view factors

performances are deteriorated and the FOS value is near to reach a level of exactly 1 or, just below the acceptable value. This suggests that with decreasing vertical spacing between neighbouring bodies, the confinement and degree of interlock and load transfer are enhanced increasing resistance to seismic sliding. The strengthening effect occurs predominantly in the shear resistance over critical failure surfaces rather than significantly influencing global deformations which are reflected by similar displacements among reinforced cases(Al-Nedawi et al., 2020).

The stress redistribution can be noticed of the three enhanced models and this is also different from that for the compacted clay model, with a more uniformly distributed stress in these three cases as well as less stress concentrated near downstream slope region. It is demonstrated that the reinforcement is able to mobilize tensile resistance in geogrids, mitigating severe shear strain localization and stabilizing natural slip planes. Better stress path contributes to enhancing FOS, and improving post-earthquake stability **(Fig 17)**(Alfatlawi et al., 2020).

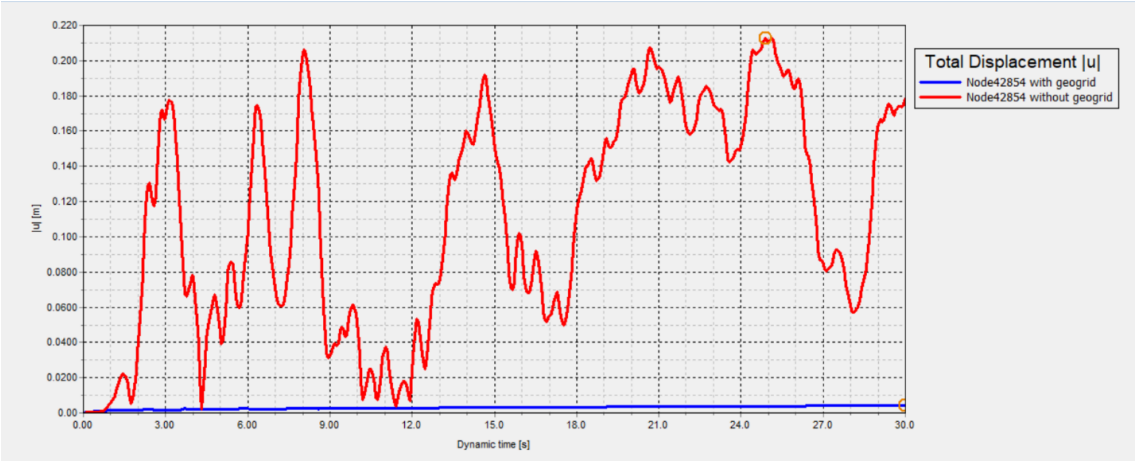

Fig 16. Comparison of time histories of total displacement magnitude |u| at the downstream monitoring node (Node 42854) for reinforced and unreinforced dam configurations under dynamic seismic loading.

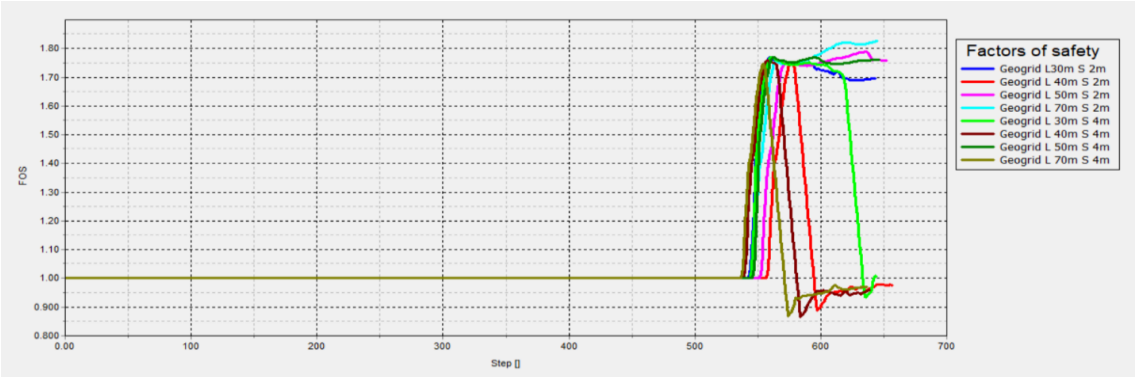

Fig 17: Comparison of factor of safety (FOS) convergence curves for different HDPE geogrid reinforcement configurations with varying embedment lengths and vertical spacings.

Comparative Discussion and Engineering Implications

The quantitative analysis for both unreinforced and reinforced sections of Al-Adhaim Dam at (EL = 143 m) under Elctrl seismic excitation (PGA = 0.3) gasmade evident that the downstream HDPE geogrid would be effective to improve about seismic behavior and safety(Ali et al., 2024). The unreinforced section meanwhile maintains a general stability state and global instability is not obvious, but its behavior features large seismic-induced displacements and concentrated deformation on the downstream slope, which may affect usage performances or long-term operational safety. All main response variables show a statistically significant improvement after strengthening. The average value of the maximum accumulated total displacement at the crucial downstream monitoring section is decreased by more than one order of magnitude, implying satisfactory inhibition on deformation localization (Ali et al., 2024). At the same time, it is observed that the factor of safety increases

uniformly well over the generally accepted seismic design value (FOS > 1.5) indicating a migration from marginal stability to robust level of security under extreme dynamic load condition. Stress redistribution in the reinforced downstream shell becomes more homogeneous, indicating improved confinement and shear resistance by geogrid layers. Such a redistrubition would ameliorate the stress concentration in proximity to precursory slip surfaces and restrict development of critical failure mechanisms. The hydromechanical response remains unaltered in either case but, whilst reinforcement only hinders strain-softening, leading to smoother deformation–seepage interaction, it does not prevent hydraulic softening and preserves effective stress conditions. Convergence pattern in **(Fig 18)** also implies that the enhanced numerical stability as well as the mechanical robustness of the reinforced formulation is achieved. The engineering and designing perspective shows that the special arrangement layer of six geogrid layers (2 m spaced vertically) with certain embedment length between 30 m and 50 m would be an optimal combination for seismic safety, deformation control, and construction economy. This arrangement brings significant performance improvement with less material spent on it, and is a highly efficient and economical structure to be applied in seismic strengthening of existing earth dams located in high-seismic-hazard areas **(Table 3)** (Rawat et al., 2023).

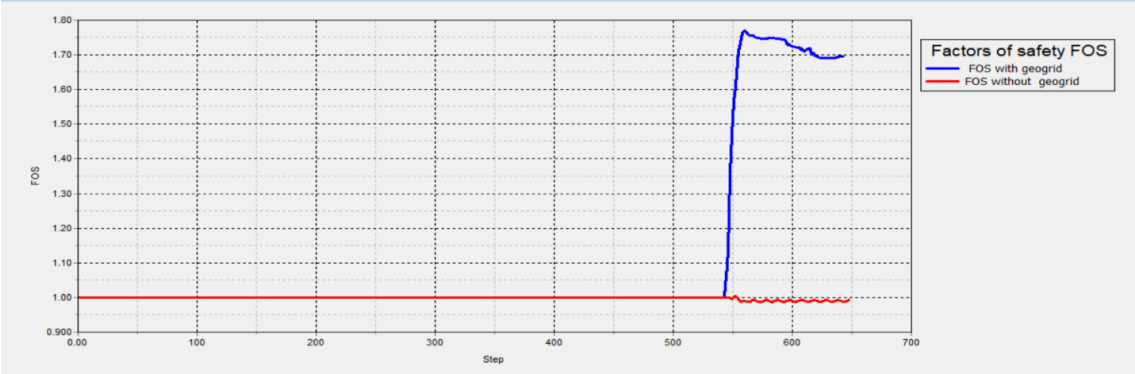

Fig 18: Comparison of factor of safety (FOS) convergence curves for reinforced and unreinforced dam configurations obtained from strength reduction analysis.

Table 4. Statistical Comparison of Seismic Performance Indicators for Unreinforced and Reinforced Al-Adhaim Dam under El-Centro Earthquake (PGA = 0.30 g, EL = 143 m)

Performance Indicator	**Unreinforced Dam**	**Reinforced Dam (Optimal Configuration)**	**Improvement Ratio / Change**
Maximum total displacement at downstream node (m)	0.211 – 0.33	(7.78 – 8.12) × 10^{-3}	↓ ~96–98%
Mean downstream displacement (m)	≈ 0.28	≈ 7.9 × 10^{-3}	↓ ~97%
Standard deviation of displacement response (m)	High (localized concentration)	Very low (uniform response)	Significant reduction
Minimum factor of safety (FOS)	≈ 1.00 – 1.18	1.696 – 1.758	↑ +45–70%
Maximum factor of safety (FOS)	≈ 1.18	≈ 1.827	↑ +55%
Stress concentration near downstream slip surface	Pronounced	Reduced and redistributed	Qualitative improvement
Excess pore pressure accumulation (kPa)	Moderate, transient	Low, transient	Marginal reduction
FOS convergence stability	Slow / oscillatory	Fast / stable	Improved numerical robustness

Conclusion

The full dynamic analysis of Al-Adhaim Dam for a severe seismic load was carried out according to the El-Centro earthquake (PGA = 0.30 g) at the highest operating reservoir level (EL = 143 m). Fully coupled flow–deformation calculations show that the unreinforced dam is not able to ensure seismic stability, and there are significant deformations of the downstream slope and local

failure mechanisms resulting in a global factor of safety less than 1.0 (FOS < 1.0). This reply acknowledges that the dam, as built, cannot be found to be safe from a seismic standpoint under the loading conditions considered. Adding downstream HDPE geogrid reinforcement significantly enhances the seismic behavior of the dam. For reinforced specimens, displacement demand is significantly reduced, where there is improved stress confinement and global stability, which continuously increases, with post-reinforcement factors of safety between 1.6 and 1.8. These values indicate a distinct positive shift from unstable or marginal stability to a performance level that meets generally adopted seismic design standards for high-hazard earth dams. ANOVA-based statistical analysis also quantitatively supports the reinforcing efficiency **(Fig. 19)**. The difference in peak seismic displacement is statistically significant ($p = 3.31 \times 10^{-5}$), further indicating that deformation mitigation of the geogrid system is achieved by the mechanical effect rather than simply being contributed to numerical variation. The factor of safety analysis also has a very low p-value ($p = 1.73 \times 10^{-8}$), strongly suggesting that systemically increased slope stability is reliable. Box-plot comparisons also reveal a clear distinction between unreinforced and reinforced responses indicating transition from unstable (FOS ≈ 0.9–1.0) to stable and reliable performance zone (FOS ≈ 1.6–1.8). 6 layers of geogrid with 2 m vertical distance and length of embedment varying from 30–50 m provide an appropriate compromise between deformation control, improvement on the stability factor and construction rate. Collectively, the findings support that downstream HDPE geogrid reinforcement is an efficient and low-cost seismic retrofit for improving the earthquake resistance of Al-Adhaim Dam, as well as similar high-hazard earth dams located in seismically active regions. Beyond its structural effectiveness, the concept of incorporating polyethylene-based reinforcement within gypsum-rich embankment zones represents a sustainable and broadly applicable solution. This approach is simple to implement, economically efficient, and capable of delivering high performance over long service lives while maintaining resistance under varying environmental and loading conditions. Owing to its adaptability, durability, and low cost, this reinforcement strategy can be extended to different types of dams and applied across multiple projects, making it a practical and sustainable seismic retrofitting option for earth dams in diverse geotechnical and seismic settings.

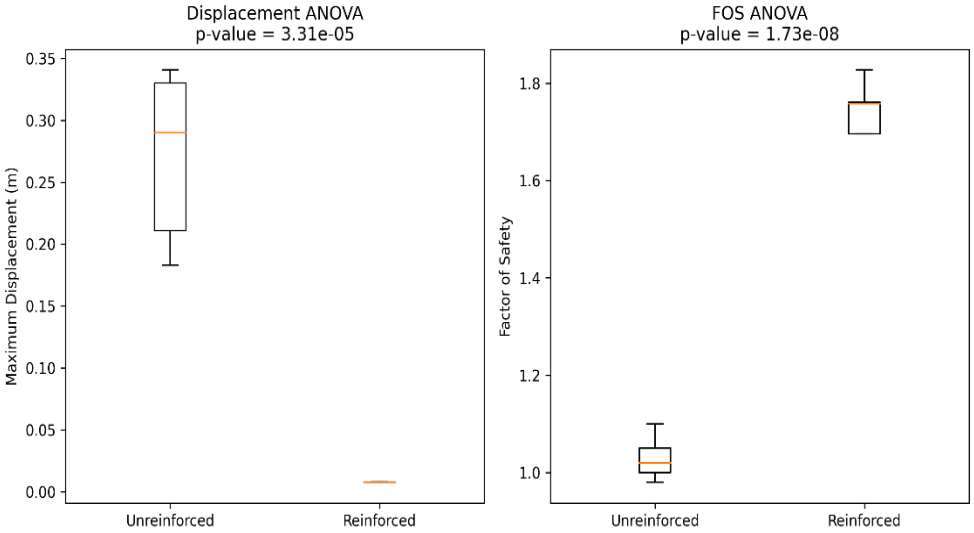

Fig 19: NOVA statistical comparison between the maximum seismic displacement and the factor of safety for different configurations for unreinforced and geogrid-reinforced at Al-Adhaim Dam subjected to El-Centro earthquake loading case (PGA = 0.30 g, EL = 143 m).

Author Contributions Conceptualization:

Iman Hameed Al-Shahrastani, Atheer Zaki Al-Qaisi. Methodology development: Iman Hameed Al-Shahrastani, Atheer Zaki Al-Qaisi. Literature review and data collection: Iman Hameed Al-Shahrastani. Analysis and interpretation of seismic deformation mechanisms: Atheer Zaki Al-Qaisi, Iman Hameed Al-Shahrastani. Preparation of figures and tables: Iman Hameed Al-Shahrastani. Writing—original draft preparation: Iman Hameed Al-Shahrastani. Writing—review and editing: Atheer Zaki Al-Qaisi. Supervision and final approval of the manuscript: Atheer Zaki Al-Qaisi. All authors have read and approved the final version of the manuscript.

Acknowledgements

The authors would like to acknowledge the support provided by the Department of Water Resources Management Engineering, College of Engineering, Al-Qasim Green University, Babylon, Iraq. The authors also appreciate the academic and technical environment that facilitated the completion of this review. No external financial funding was received specifically for this study.

Funding:

This study was carried out without any external financial support

Conflicts of Interest

The authors declare that there are no conflicts of interest regarding the publication of this paper.

References

Abbas, I. H., & Al-Hadidi, M. T. (2021). Effect of Halabjah earthquake on Al-Wand earth dam: Numerical analysis. E3S Web of Conferences, 263, Article 01016. EDP Sciences.

Adamo, N. (1985). Earthquakes and their effects on embankment dams. Iraq Journal of Water Resources. Ministry of Irrigation.

Adamo, N. (1985). Earthquakes and their effects on embankment dams. Iraq Journal of Water Resources. Ministry of Irrigation.

Akbaş, B. (2015). Probabilistic slope stability analysis using limit equilibrium, finite element and random finite element methods (Master's thesis). Middle East Technical University.

Al-Amshawee, M. A. H. (2014). Behavior of earth dams during rapid drawdown of reservoir (Master's thesis). Building and Construction Engineering Department, Water Resources Branch, University of Technology.

Alfatlawi, T. J., Al-Temimi, Y. K., & Alomari, Z. M. (2020). Evaluation of the upstream slope stability of earth dams based on drawdown conditions: Khassa Chai dam as a case study. IOP Conference Series: Materials Science and Engineering, 881, Article 012072. IOP Publishing.

Al-Hadidi, M. T., & Hashim, S. (2021). Finite element analysis of seepage for Kongele earth dam using GEO-STUDIO software. Journal of Physics: Conference Series, 1973, Article 012003. IOP Publishing.

Al-Janabi, A. M. S., Ghazali, A. H., Ghazaw, Y. M., Afan, H. A., Al-Ansari, N., & Yaseen, Z. M. (2020). Experimental and numerical analysis for earth-fill dam seepage. Sustainability, 12(6), Article 2490.

Al-Jaroosh, M. G. M. (2014). Effect of horizontal drain size on the stability of earth dams in steady seepage conditions (Master's thesis). University of Technology.

Al-Labban, S. N. Y. (2007). Seepage analysis of earth dams by finite elements (Master's thesis). University of Kufa.

Al-Nedawi, N. M., & Al-Hadidi, M. T. (2020). Finite element analysis of seepage for Hemrin earth dam using GEO-STUDIO software. Diyala Journal of Engineering Sciences, 66–76.

Chimdesa, F. F., Jilo, N. Z., Hulagabali, A., Babalola, O. E., Tiyasha, T., Ramaswamy, K., Kumar, A., & Bhagat, S. K. (2023). Numerical analysis of pile group, piled raft, and footing using finite element software PLAXIS 2D and GEO5. Scientific Reports, 13(1), Article 15875. https://doi.org/10.1038/s41598-023-15875-x

Fallah, H., & Noferesti, H. (2015). Stability assessment of the Farrokhi earth embankment dam using the pseudo-static and deformation-based methods. International Journal of Mining and Geo-Engineering, 49(2), 205–220.

Ghalib, H. A., & A., S. A. (1974). Seismotectonics of the Arabian Peninsula: A global tectonic approach.

Hussain, H. H., Al Obaidy, A. I., Hommadi, A. H., Al Hudaib, H. T., Al Masoodi, A. T., Saeed, F. H., & Al Saeedi, N. N. (2022). Modifying the spillway of Adhaim Dam, reducing flood impact, and saving water. Journal of Water Management Modeling.

IMOS. (2023). Seismic activity map. General Authority for Meteorology and Seismic Monitoring, Ministry of Transportation, Baghdad, Iraq.

Ministry of Water Resources (MOWR). (1994). Final report of Al-Adhaim earth dam. College of Engineering, University of Baghdad.

Mousa, S., & Boshnaq, M. H. SEEPAGE ANALYSIS OF A ZONED EARTH DAM BY FINITE ELEMENTS.

Novak, P., Moffat, A., Nalluri, C., & Narayanan, R. (2007). Hydraulic structures. CRC Press.

Novak, P., Moffat, A., Nalluri, C., & Narayanan, R. (2017). Hydraulic structures. CRC Press.

PLAXIS. (2020). PLAXIS 2D reference manual (Version 20). Bentley Systems.

Talukdar, P., & Barman, N. (2012). Seismic activity and seismotectonic correlation with reference to Northeast India. IOSR Journal of Applied Physics, 2(2), 24–29.

U.S. Army Corps of Engineers (USACE). (2003). Engineering and design: Slope stability (Engineer Manual EM 1110-2-1902). Department of the Army, Washington, DC.